



Novel dye sensitizers of main chain polymeric metal complexes based on complexes of diaminomaleonitrile with Cd(II), Ni(II): Synthesis, characterization, and photovoltaic performance for dye-sensitized solar cells

Wei Zhang, Xueliang Jin, Xiaoguang Yu, Jun Zhou, Guipeng Tang, Dahai Peng, Jiaomei Hu, Chaofan Zhong*

Key Laboratory of Environmentally Friendly Chemistry and Applications of Ministry of Education, College of Chemistry, Xiangtan University, Xiangtan, Hunan 411105, China

ARTICLE INFO

Article history:

Received 22 June 2013

Received in revised form

27 August 2013

Accepted 5 September 2013

Keywords:

Dye-sensitized solar cells

Polymeric metal complex

Thiophene

Diaminomaleonitrile

Photovoltaic performance

ABSTRACT

Four new donor- π -acceptor (D- π -A) dyes (**P1**, **P2**, **P3**, **P4**) were synthesized, characterized and applied in dye-sensitized solar cells (DSSCs). Poly(*p*-phenylenevinylene) (PPV) or Bisthien PPV was used as donor, ethilenic link or thiophene as π -bridge, and Cadmium complexes or Nickel complexes as acceptor in these D- π -A type sensitizers. The introduction of the polymerization of π system and the metal complexes has greatly increased the light absorption. Increasing the number of thienyl group in the molecule to a certain extent was effective in further lowering both the highest occupied molecular orbital (HOMO) and the lowest unoccupied molecular orbital (LUMO) energy levels to attain higher open-circuit voltage (V_{oc}). Among them, **P3**-based cell shows excellent photovoltaic performance and power conversion efficiency up to 2.25% under AM 1.5G irradiation (100 mW cm^{-2}).

© 2013 Elsevier B.V. All rights reserved.

1. Introduction

Solar cells, or photovoltaics, were recognized as the main methods and approaches to solve the world's future energy problems [1]. Since 1954, Chapin, Fuller, and Pearson at Bell Laboratories have improved the efficiency of a Si cell to 6% [2]. Especially in the last twenty years, the research and practical applications of solar cells have made a lot of progress. But it can not also compete with fossil fuels on the issues of cost and practicality. At present, the research and applications of solar cells have been to enter the third generation [3,4]. The first generation is crystalline silicon solar cells, whose energy conversion efficiency can reach 24%, but the cost is more than 3 \$ per peak watt (Wp); The second generation solar cells, for example, amorphous silicon, CIGS, and CdTe, are based on thin film technologies, whose energy conversion efficiency was up to 19%, and the cost was down to 1 \$ per peak watt (Wp) [5]. In order to further reduce the costs and investments, scientists have embarked on the third generation organic solar cells. The goal for

the third generation solar cells is to deliver electricity at a large scale competitive price, that is, less than 0.5 \$/Wp, which can complete with fossil energy. From the current point of research progress, Dye-sensitized solar cells will be the most potential third-generation solar cells.

Dye-sensitized solar cells (DSSCs), also known as Grätzel cells, were invented by Grätzel and O'Regan in 1991 [6]. There are more advantages of dye-sensitized solar cells than the first-generation and second-generation solar cells: relatively small weight; low production cost; short energy payback time; high light-to-electrical conversion efficiencies, and so forth [7–9]. The key indicator to measure the performance of dye-sensitized solar cells is the conversion efficiency. The theoretical conversion efficiency could be achieved about 20%, but the maximum efficiency of the current experimental study is just 12% [10,11]. There are a lot of factors that affect the conversion efficiency of the solar cells, and the photosensitizer is one of the most critical parts in dye-sensitized solar cells, because it determines the light absorption properties, electron transport, and the composite performance. Therefore, many scientists of chemistry, physics and materials take much interest in the new high-performance dye sensitizers, and it has become the most favorite of worldwide research and development applications.

* Corresponding author.

E-mail addresses: zhongcf798@aliyun.com, zhongcf798@yahoo.com.cn (C. Zhong).

Thousands of dyes have been synthesized and tested in DSSCs so far, and it can be divided into three categories. The first type of dye sensitizer is metal complexes, especially the ruthenium (Ru(II)) complexes. Light absorption in the visible part of the solar spectrum is due to a metal to ligand charge transfer (MLCT) process [12]. Among them, the most prominent is **N719** and **N749**, and their efficiency could be reached to 10.4% and 11.1%, respectively [13]. As we all know, rare metal ruthenium is very expensive and pollute environment badly. Therefore, it is difficult to continue the breakthrough and development.

The second type of dye sensitizers is porphyrin and phthalocyanine. Because they exhibit intense spectral response bands in the near-IR region and possess good chemical, optical and thermal stability. However, the energy conversion efficiency has been hovering around 3%–9% [14–17]. Until 2010 and 2011, also the Grätzel team synthesized the zinc porphyrin **YD2** [18], **YD2-o-C8** [19], the energy conversion efficiency of 11.2% and 12.7% of the record. Owing to the poor solubility of such dyes, it is difficult for film formation on the surface of the TiO₂, so its development will also be restricted.

The third type of sensitizers is organic dyes. They include n-type dyes such as coumarin dyes [20–22], triphenylamine dyes [23,24], carbazole dyes [25–27], perylene dyes [28–30], and p-type dyes [31,32]. Compared with the noble ruthenium complex dyes, organic dyes have many advantages: structure diversity, easy design and synthesis, low cost, fewer environmental pollution problems, high extinction coefficient, and a higher conversion efficiency of 5%–10% [33]. The organic dyes have poor chemical stability, light stability, especially the thermal stability due to a small molecular weight. Therefore, it is difficult to achieve large-scale research and application.

People have come up to a preliminary conclusion on the dyes' synthesis from the research and development of the above dye sensitizers in order to obtain more efficient dye sensitizers. To design a new dye, we should bear in mind the following rules: wide absorption band and a high absorption coefficient; favorable HOMO and LUMO energies for efficient charge transfer; a good carrier transport bridges to enhance the carrier transport; good solubility; strong anchoring on the surface of TiO₂; a high light stability, chemical stability and thermal stability for durable devices and so on. The first three features are the most important, and mainly depend on the dye molecules to the light absorption and electron transfer. This can be changed by tuning its ground state, the excitation state energy and the energy gap ΔE ($\Delta E = E$ excited state – E ground state). In order to reduce the ΔE of a given dye (Low band gap of metallated polymer can extend toward the near-infrared (NIR) range of the solar spectrum [34,35]), thereby shifting the λ_{\max} to longer wavelengths, the following major approaches can be adopted: (i) enlargement of the π systems, (ii) transition from aromatic to quinoidal structures, (iii) introduction of donor acceptor substituents, (iv) polymerization.

It is well known that metal chelates of salicylaldehyde and diaminomaleonitrile (DAMN) derivatives are the most super materials as an electron transporter, and increasing the number of thiophene units in poly(*p*-phenylenevinylene) can further extend the π -conjugation, which can also increase the short circuit photocurrent, as the result of the red-shifted absorption of the sensitizer loaded TiO₂ film [36]. Although chemists rarely report their application as dye sensitizers for dye-sensitized solar cells, there is no doubt that polymeric substance contains salicylaldehyde and DAMN may satisfy application requirements to make an effective way to improve open-circuit photovoltage (V_{oc}).

According to the above-mentioned points, we have designed and synthesized four D- π -A dyes possessing a metal-DAMN as an acceptor (A), ethilenic bond as a π -conjugation linkage, and poly(*p*-

phenylenevinylene) (PPV) or bithiophene phenylenevinylene as donor group (D), which are shown in Scheme 1. The work of Wong et al. offers an attractive avenue towards conjugated materials with broad solar absorptions and demonstrates the potential of metallopolyyenes for both visible and NIR light power generation [37,38]. Moreover, thermal properties, optical properties, and photovoltaic properties of polymeric metal complexes are also investigated in this paper.

2. Experimental section

2.1. Materials

NiCl₂(PPh₃)₂, diaminomaleonitrile (DAMN) and 3-methyl-2-thiophenecarboxaldehyde were obtained from Aldrich Chemical Co. and used as received. *N,N*-Dimethylformamide was dried by distillation over CaH₂, and methanol was dried over molecular sieves and freshly distilled prior to being used. The other materials were common commercial grade and used as received. All chemicals used were of an analytical grade. Solvents were purified with conventional methods.

2.2. Instruments and measurements

¹H NMR were performed in CDCl₃ and recorded on a Bruker Avance 400 spectrometer. Gel Permeation Chromatography (GPC) analyses were measured by a WATER 2414 system equipped with a set of HT₃, HT₄ and HT₅, 1-styragel columns with THF as eluent and polystyrene as standard. The FT-IR spectra were obtained on a Perkin–Elmer Spectrum. One Fourier transform infrared spectrometer by incorporating samples in KBr pellets. Differential Scanning Calorimetry (DSC), Thermogravimetric analysis (TGA) and Elemental analysis were performed on Perkin–Elmer DSC-7 thermal analyzer, Shimadzu TGA-7 Instrument, and Perkin–Elmer 2400 II instrument, respectively. UV–Visible spectra of all the polymers were taken on a Lambda 25 spectrophotometer. Photoluminescent spectra (PL) were taken on a Perkin–Elmer LS55 luminescence spectrometer with a xenon lamp as the light source. Cyclic voltammetry (CV) was conducted on a CHI630C Electrochemical Workstation using a three electrode system, in a [Bu₄N]BF₄ (0.1 M) DMF solution at a scan rate of 100 mV/s. A glassy carbon rod, a Pt wire electrode and a saturated calomel electrode (SCE) were used as working electrode, auxiliary electrode and reference electrode, respectively.

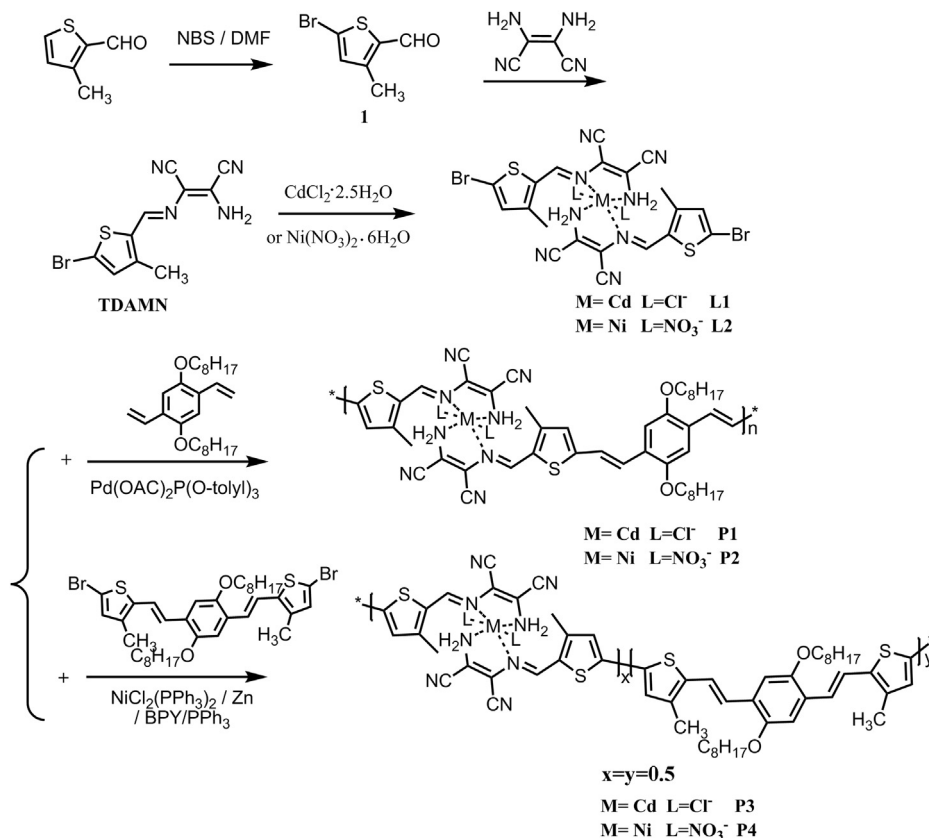
2.3. Synthesis

2.3.1. Synthesis of 5-bromo-3-methyl-2-thiophenecarboxaldehyde (**1**)

Following the preparation as described in U.S. Publication NO. 2006/0199836, Br₂ (7.34 mL, 0.14 mol) was added to a solution of 3-methyl-2-thiophenecarboxaldehyde (17.1 mL, 0.14 mol) in chloroform (118 mL) dropwise at 0 °C over a period of 20 min. The reaction was allowed to slowly warm to room temperature and stir for 2 h. The brown/red solution was diluted with 150 mL of CH₂Cl₂ and washed with water, 1.5 M K₂HPO₄ and brine. The organic layer was dried over anhydrous Na₂SO₄ and concentrated. The residue was purified by flash chromatography (silica gel, hexanes:EtOAc, 100:0–50:50) to afford 25.1 g (65% yield) of the title compound as a brown solid: ¹H NMR (400 MHz, CDCl₃) 9.94 (s, 1H), 6.74 (s, 1H), 2.58 (s, 3H).

2.3.2. Synthesis of (2-amino-3-(5-bromo-3-methylthiophen-2-yl)methyleneamino)-fumarionitrile (**TDAMN**)

An ethanol solution (100 mL) of 5-bromo-3-methyl-2-thiophenecarboxaldehyde (**1**) (2.0326 g, 0.01 mol) was dropped



Scheme 1. Synthetic route of the monomers and polymeric metal complexes **P1–P4**.

to an ethanol solution (20 mL) of DAMN (1.0810 g, 0.01 mol), and the mixture was refluxed for 16 h. The yellow solution was cooled in ice to give fine yellow needles, which were filtered off, washed with cooled ethanol, and dried under vacuum (2.2137 g yield 75%). FT-IR (KBr, cm^{-1}): 3406, 3299, 3196, 2234, 2202, 1616, 1589, 1420, 1381, 824. Anal. Calcd for $\text{C}_{10}\text{H}_7\text{BrN}_4\text{S}$ (**2**): C, 40.69; H, 2.39; N, 18.98; S, 10.86. Found: C, 41.35; H, 2.24; N, 19.47; S, 11.42. MS: Calcd for $\text{C}_{10}\text{H}_7\text{BrN}_4\text{S} [\text{M}]^+$ 293.96; found, 294.95. ^1H NMR (400 MHz, CDCl_3): 7.62 (s, 1H), 6.74 (s, 1H), 2.35 (s, 2H), 2.21 (s, 3H).

2.3.3. Synthesis of **L1** [39]

$\text{CdCl}_2 \cdot 2.5\text{H}_2\text{O}$ (0.0572 g, 0.25 mmol) was dissolved in methanol (50 mL) with stirring and refluxing. 2-amino-3-(*E*)-(5-bromo-3-methylthiophen-2-yl)methyl-ene-amino-fumaronitrile (**2**) (0.1476 g, 0.5 mmol) dissolved in methanol (75 mL) was then added and the mixture refluxed for 11 h to give a khaki-brown precipitate, which was filtered off, washed with methanol, and dried under vacuum. Yield: 0.1794 g (93%). Anal. Calcd for $\text{C}_{20}\text{H}_{12}\text{Br}_2\text{Cl}_2\text{N}_8\text{S}_2\text{Cd}$: C, 31.13; H, 1.57; N, 14.52; S, 8.31. Found: C, 31.54; H, 1.62; N, 13.98; S, 8.39. FT-IR (KBr, cm^{-1}): 3040 ($=\text{C}-\text{H}$), 2976, 2919, 1570 ($\text{C}=\text{N}$), 2175 ($\text{C}\equiv\text{N}$), 1035 ($\text{C}-\text{O}-\text{M}$), 931 ($\text{Ar}-\text{H}$), 494 ($\text{N}-\text{M}$).

2.3.4. Synthesis of **L2**

In the same manner as described for **L1** afford a light brown solid. Yield: 91%. Anal. Calcd for $\text{C}_{20}\text{H}_{12}\text{Br}_2\text{N}_{10}\text{O}_6\text{S}_2\text{Ni}$: C, 31.16; H, 1.57; N, 18.17; S, 8.32, 14.52. Found: C, 30.82; H, 1.62; N, 18.24; S, 8.40. FT-IR (KBr, cm^{-1}): 3038 ($=\text{C}-\text{H}$), 2973, 2931, 1642, 1569 ($\text{C}=\text{N}$), 2427 ($\text{C}\equiv\text{N}$), 1030 ($\text{C}-\text{O}-\text{M}$), 939 ($\text{Ar}-\text{H}$), 492 ($\text{N}-\text{M}$).

2.3.5. Synthesis of polymeric metal complex **P1**

The polymeric metal complex **P1** was synthesized by using the Heck coupling method, according to the literature [40]. A flask was

charged with a mixture of metal complex **L1** (0.2315 g, 0.3 mmol), 1,4-bis(octyloxy)-2,5-divinylbenzene (0.116 g, 0.3 mmol), $\text{Pd}(\text{OAc})_2$ (0.0024 g, 0.012 mmol), triethylamine (3 mL), 3-*o*-tolyl phosphine (0.0220 g, 0.072 mmol) and DMF (8 mL). Then the flask was pumped into a vacuum and purged with N_2 . The mixture was heated at 90°C for 18 h under N_2 . After that, it was filtered after cooled to room temperature and the filtrate was poured into ethanol. The yellow precipitate was filtered and washed with cold ethanol. The crude product was purified by dissolving in DMF and precipitating into ethanol to afford a light yellow solid. (Yield: 0.2965 g, 56%). FT-IR (KBr, cm^{-1}): 2921, 2851, 1643 ($\text{C}=\text{N}$), 2328 ($\text{C}\equiv\text{N}$), 1095 ($\text{C}-\text{O}-\text{M}$), 784 ($\text{Ar}-\text{H}$), 495 ($\text{N}-\text{M}$). Et al. Calcd for $[\text{C}_{46}\text{H}_{52}\text{Cl}_2\text{N}_8\text{O}_2\text{S}_2\text{Cd}]$: C, 55.45; H, 5.26; N, 11.25; S, 6.44. Found: C, 56.21; H, 5.73; N, 11.32; S, 6.92. Mn = 13.0 kg/mol, PDI = 1.31.

2.3.6. Synthesis of polymeric metal complex **P2**

With the similar synthetic method as **P1** afford a yellow solid (0.1807 g, 52%). FT-IR (KBr, cm^{-1}): 2928, 2849, 1657 ($\text{C}=\text{N}$), 2355 ($\text{C}\equiv\text{N}$), 1108 ($\text{C}-\text{O}-\text{M}$), 762 ($\text{Ar}-\text{H}$), 496 ($\text{N}-\text{M}$). Et al. Calcd for $[\text{C}_{46}\text{H}_{52}\text{N}_{10}\text{O}_8\text{S}_2\text{Ni}]$: C, 55.48; H, 5.26; N, 14.07; S, 6.44. Found: C, 56.03; H, 5.75; N, 14.71; S, 6.02. Mn = 11.9 kg/mol, PDI = 1.36.

2.3.7. Synthesis of polymeric metal complex **P3**

The copolymer was synthesized by Yamamoto coupling method according to the lit [41,42]. **L1** (0.1543 g, 0.2 mmol), bis(triphenylphosphine) nickel(II) chloride (0.13 g, 0.2 mmol), 2,2'-(2,5-bis(octyloxy)-1,4-phenylene)bis(ethene-2,1-diyl)bis(2-bromo-4-methylthiophene) (0.1474 g, 0.2 mmol), zinc (0.065 g, 1 mmol), triphenylphosphine (0.1045 g, 0.4 mmol), and a little bipyridine (0.003 g, 0.019 mmol) were dissolved in DMF (7.5 mL) under nitrogen. Then the mixture was stirred at 90°C for 48 h. The yellow

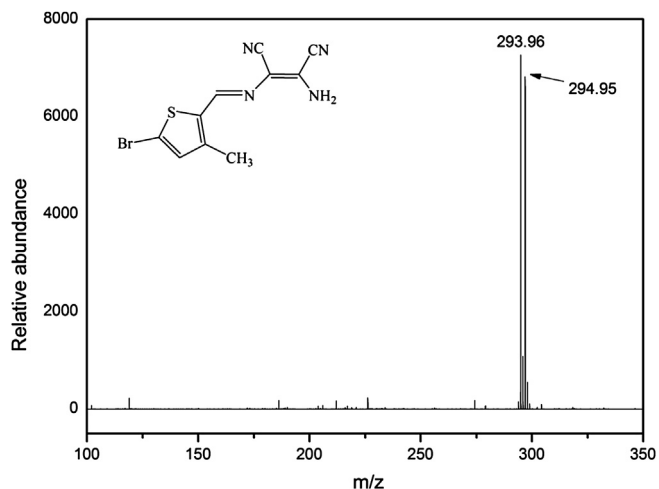


Fig. 1. Time-of-flight mass spectrometry of (TDAMN).

solid was precipitated into a large excess of ethanol solution. The crude product was washed with ethanol, distilled water, and THF sequentially, then dried in vacuum at 65 °C for one day to afford pale yellow solids (0.1480 g, 61%). FT-IR (KBr, cm^{-1}): 3051 ($=\text{C}-\text{H}$), 2924, 2862, 1645 ($\text{C}=\text{N}$), 2210 ($\text{C}\equiv\text{N}$), 1113 ($\text{C}-\text{O}-\text{M}$), 761 ($\text{Ar}-\text{H}$), 497 ($\text{N}-\text{M}$). Anal. Calcd for $[\text{C}_{56}\text{H}_{60}\text{Cl}_2\text{N}_8\text{O}_2\text{S}_4\text{Cd}]$: C, 56.58; H, 5.09; N, 9.43; S, 10.79. Found: C, 57.12; H, 4.56; N, 9.51; S, 10.82. $\text{Mn} = 10.7$ kg/mol, PDI = 1.67.

2.3.8. Synthesis of polymeric metal complex **P4**

With the similar synthetic method as **P3** afford a yellow solid. Yield (%): 63%. FT-IR (KBr, cm^{-1}): 3049 ($=\text{C}-\text{H}$), 2915, 2856, 1659 ($\text{C}=\text{N}$), 2217 ($\text{C}\equiv\text{N}$), 1115 ($\text{C}-\text{O}-\text{M}$), 719 ($\text{Ar}-\text{H}$), 494 ($\text{N}-\text{M}$). Anal. Calcd for $[\text{C}_{56}\text{H}_{60}\text{N}_{10}\text{O}_8\text{S}_4\text{Ni}]$: C, 56.61; H, 5.09; N, 11.79; S, 10.80. Found: C, 57.25; H, 6.57; N, 11.68; S, 10.37. $\text{Mn} = 9.5$ kg/mol, PDI = 1.53.

3. Results and discussion

3.1. Synthesis and characterization

The detailed synthetic routes of the four polymeric metal complexes (**P1**, **P2**, **P3**, **P4**) as well as the monomers are shown in Scheme 1. Meanwhile, the two polymers (**P1**, **P2**) were synthesized by the Heck coupling [43], the other two polymers (**P3**, **P4**) were synthesized by the Yamamoto coupling [41]. The four as-synthesized polymers could be dissolved in common organic solvents such as DMF and THF at room temperature. But in the other solvents they exhibit a poor solubility, such as in acetone and chloroform.

Fig. 1 shows time-of-flight mass spectrometry of (TDAMN), $[\text{M}]^+$ 293.96; found, 294.95. It indicates that the compound has been successfully synthesized (Fig. 2 ^1H NMR spectra of TDAMN in CDCl_3 solution).

The IR spectra of the ligand monomer (**2**), metal complex (**L1**, **L2**) and the target polymers (**P1**, **P2**, **P3**, **P4**) are shown in Figs. 3 and 4. As for the monomer **2**, the absorption peaks at 3406, 3299, 3196 cm^{-1} are the characteristic absorption peaks of the amino-group stretching vibration, absorption peaks at 2234, 2202 are due to $\text{C}\equiv\text{N}$ bond stretching vibration, absorption peaks at 1616 cm^{-1} are due to $\text{C}=\text{N}$ bond stretching vibration, and 1590 is the bond stretching vibration of $\text{C}=\text{C}$. From Figs. 3 and 4, the peaks of 1035 cm^{-1} and 1030 cm^{-1} are due to $\text{C}-\text{N}-\text{M}$ stretching vibration of metal compound **L1** and **L2** respectively [44]. And then integrating with the results of elemental analysis, we can come up with that metal Cd^{2+} and Ni^{2+} which have been successfully coordinated with ligand **2**, namely, complexes **L1** and **L2** have been successfully synthesized.

Gel permeation chromatography (GPC) study for all the target polymers is shown in Table 1. The number average molecular weight of **P1**, **P2**, **P3** and **P4** are 13.0, 11.9, 10.7 and 9.5 kg/mol, and the units of them are 13, 12, 9 and 8 respectively. All the PDI of polymeric metal complexes are relatively wide (**P1**, **P2**, **P3**, **P4**: 1.31, 1.36, 1.67 and 1.53, respectively). The changes of the molecular weight are also proved that the copolymerization has been taken

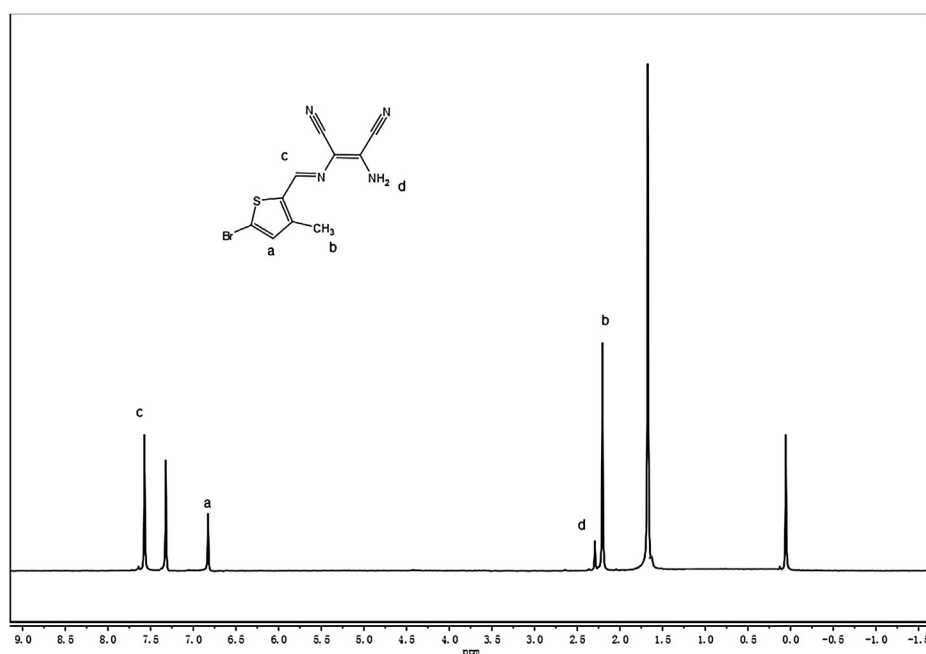


Fig. 2. ^1H NMR spectra of TDAMN in CDCl_3 solution.

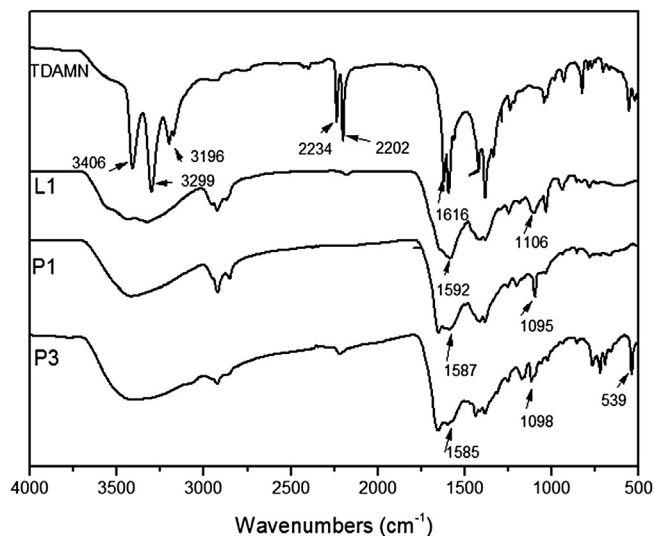


Fig. 3. FT-IR spectra of TDAMN, L1, P1, P3.

place between the monomers, which is a further evidence for the target polymers that have been successfully synthesized.

3.2. Optical properties

The UV–vis and normalized PL spectra of the polymeric metal complexes **P1**, **P2**, **P3** and **P4** (10^{-5} M in DMF solution) are shown in Figs. 5 and 6 respectively, and the corresponding data are summarized in Table 2.

The ligand **L** shows a UV–vis normalized absorption peak located at about 350 nm, corresponding to the $\pi-\pi^*$ electron transitions of the conjugated molecules, which was observed in the ICT between the electron acceptor TDAMN unit and the electron donating PPV moiety. In Fig. 5, the maximum absorption of **P1**, **P2**, **P3** and **P4** are at 420, 405, 451 and 422 nm, respectively. Those polymers have very weak shoulder absorption peak in the band 450–550 nm due to the charge transition of the DAMN derivatives and d^{10} metal ions in the polymer. The one which shows a better UV absorption by comparing **P2** with **P4** as well as **P1** with **P3**, indicates that polymers containing metal-Cd have better absorption

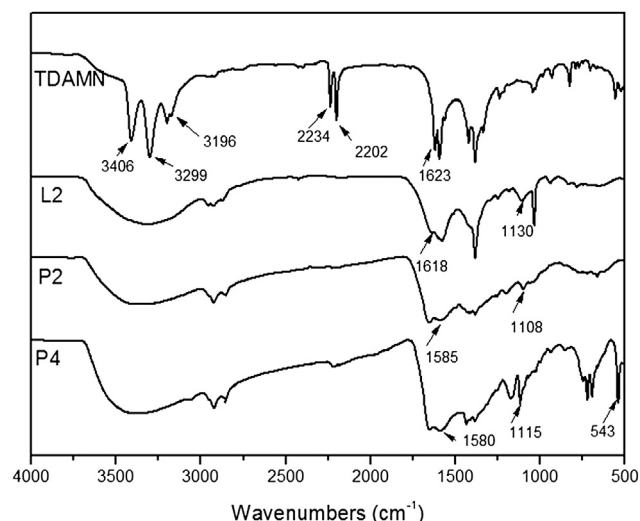


Fig. 4. FT-IR spectra of TDAMN, L2, P2, P4.

Table 1
Molecular weights and thermal properties of the polymeric metal complexes.

Polymer	\bar{M}_n^a [$\times 10^3$]	\bar{M}_w^a [$\times 10^3$]	PDI	T_g^b [$^{\circ}\text{C}$]	T_d^c [$^{\circ}\text{C}$]
P1	13.0	17.0	1.31	153	325
P2	11.9	16.2	1.36	131	302
P3	10.7	17.9	1.67	144	353
P4	9.5	14.5	1.53	120	330

^a Determined by gel permeation chromatography using polystyrene as standard.

^b Determined by DSC with a heating rate of $20^{\circ}\text{C}/\text{min}$ under nitrogen.

^c The temperature at 5% weight loss under nitrogen.

of light than polymers containing metal-Ni. And it also indicates that adding thienyl group into polymers can promote the absorption of light.

The normalized photoluminescent (PL) spectra of **P1**, **P2**, **P3** and **P4** in DMF solution are shown in Fig. 6, the excitation wavelengths were set according to the absorption peak of UV–vis spectrum, and the corresponding optical data are also listed in Table 2. It can be seen that the PL peaks of them are at 486, 497, 455 and 470 nm, respectively, which can be attributed to the $\pi-\pi^*$ transition of intra-ligand.

3.3. Thermal stability

The thermal properties of the polymeric metal complexes were investigated by differential scanning calorimetric (DSC) and thermo-gravimetric analysis (TGA), and the corresponding data are also reported in Table 1. The TGA image which present in Fig. 7 shows that **P1**, **P2**, **P3** and **P4** possess good thermal stability with 5% weight loss at temperatures (T_d) of 325, 302, 353, and 330°C in nitrogen, respectively. We could see that **P1**, **P2**, **P3** and **P4** have glass transition temperature (T_g) ranged from 120 to 153°C and followed the order **P1** > **P3** > **P2** > **P4**, which suggests that polymeric metal complex containing metal-Cd has hold higher rigidity than that containing metal-Ni.

3.4. Electrochemical properties

The electrochemical behaviors of the polymers were investigated by cyclic voltammetry, which is one of the important properties for organic materials used in solar cells. Fig. 8 shows the cyclic voltammetry curves of **P1**, **P2**, **P3**, **P4**. The cyclic voltammetry was measured in DMF solution which used $[\text{Bu}_4\text{N}]\text{BF}_4$ as supporting electrolyte and a saturated calomel electrode (SCE) as the reference electrode with a scan rate of $100\text{ mV}/\text{s}$. The lowest unoccupied molecular orbital (LUMO), highest occupied molecular orbital (HOMO) energy levels and energy gap (E_g) can be handled conveniently by equations as follows [42].

Table 2
Optical and electrochemical properties of the polymeric metal complexes.

Polymer	$\lambda_{a,\text{max}}^a$, $\lambda_{a,\text{onset}}$	$\lambda_{p,\text{max}}^b$	$E_{g,\text{opt}}/\text{eV}^c$	E_{ox} (V) ^d	E_{red} (V) ^d	HOMO (eV)	LUMO (eV)	$E_{g,\text{EC}}/\text{eV}^e$
P1	420, 561	486	2.21	1.11	-0.92	-5.51	-3.48	2.03
P2	405, 528	497	2.35	1.06	-1.04	-5.46	-3.36	2.10
P3	451, 585	455	2.12	1.17	-0.82	-5.57	-3.58	1.99
P4	422, 566	470	2.19	1.12	-0.89	-5.52	-3.51	2.01

^a $\lambda_{a,\text{max}}$, $\lambda_{a,\text{onset}}$: The maxima and onset absorption from the UV–vis spectra in DMF solution.

^b $\lambda_{p,\text{max}}$: The PL maxima in DMF solution.

^c $E_{g,\text{opt}}$: Optical energy band gap calculated from the formula $E_g = 1240/\lambda_{a,\text{onset}}$ (eV).

^d Values determined by cyclic voltammetry.

^e $E_{g,\text{EC}}$: Electrochemical band gap estimated from HOMO and LUMO.

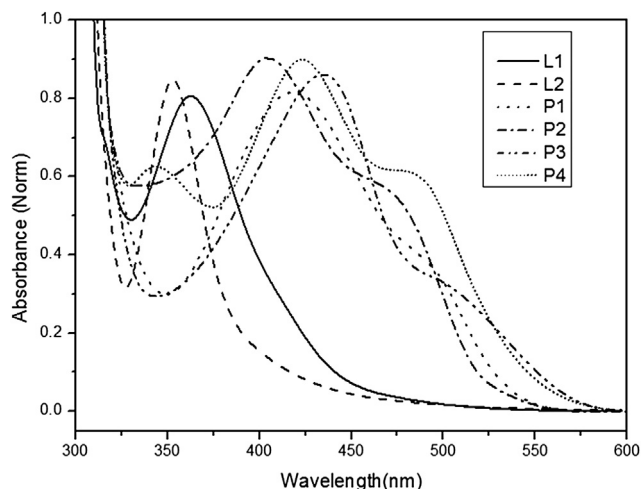


Fig. 5. UV-vis absorption spectra of **L1**, **L2** and polymeric metal complexes **P1–P4** in DMF solution.

$$\text{HOMO} = -e(E_{\text{ox}} + 4.40) \text{ (eV)} \quad (1)$$

$$\text{LUMO} = -e(E_{\text{red}} + 4.40) \text{ (eV)} \quad (2)$$

$$E_g = \text{HOMO} - \text{LUMO} \quad (3)$$

The units of E_{ox} and E_{red} are measured through electrochemical curve and the data obtained are listed in Table 3. The reduction and oxidation potentials of **P1** were measured to be $E_{\text{ox}} = 1.11$ V and $E_{\text{red}} = -0.92$ V, respectively. The energy value of the HOMO was calculated to be -5.512 eV, and the energy value of the LUMO was calculated to be -3.48 eV, so the energy band gap was 2.03 eV. In the same way, we can get the related data of other polymers. The E_g of the complexes follows the order, **P3** > **P4** > **P1** > **P2**, so **P3** is more suitable for fabrication of optoelectronic devices than **P4**, **P1** and **P2**, because a relatively low E_g can absorb light efficiently, it's very important to improve power conversion efficiency [45].

3.5. Photovoltaic properties

Fig. 10 displays the irradiation source for the photocurrent density–voltage (J – V) measurement of the DSSCs devices based on

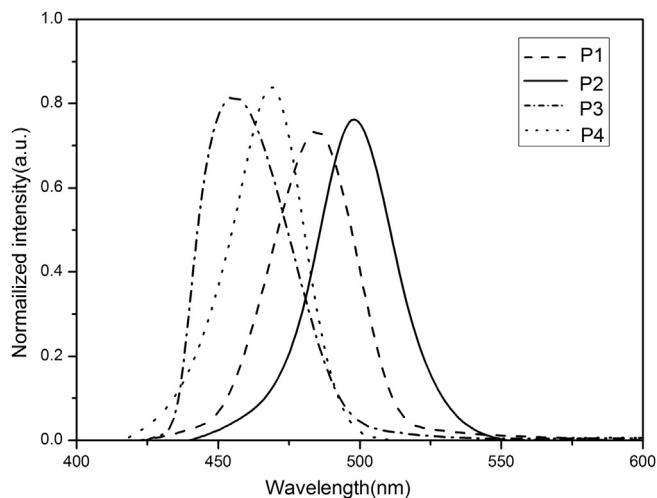


Fig. 6. PL spectra of the four polymeric metal complexes in DMF solution.

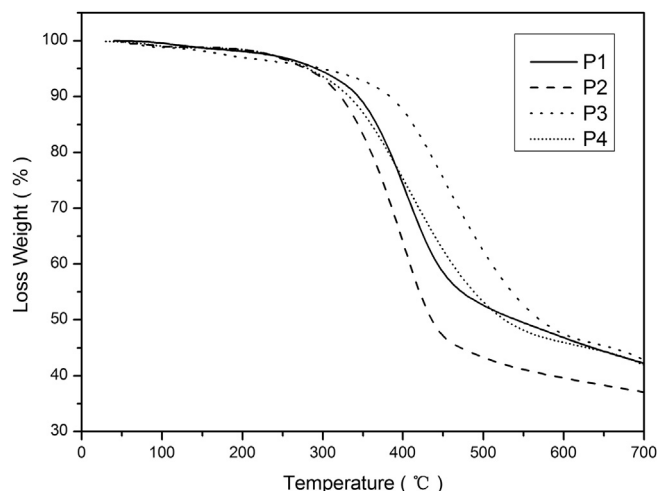


Fig. 7. TGA curves of **P1–P4** with a heating rate of 20 °C/min under nitrogen atmosphere.

the four polymeric metal complexes. Measurement of DSSCs merits such as corresponding open-circuit voltage (V_{oc}), short-circuit current density (J_{sc}), fill factor (ff), and power conversion efficiency (η) are listed in Table 3. It can be seen from the table that the V_{oc} values of **P1**, **P2**, **P3** and **P4** are 0.65, 0.61, 0.72 and 0.71, respectively. The corresponding ff values could be achieved a higher level about 70%. However, the J_{sc} values increased from 4.19 mA/cm² for **P2** to 4.75 mA/cm² for **P3**. The power conversion efficiency based on **P3** reached 2.25%, which is the highest of the device based on those four polymeric metal complexes.

The low J_{sc} is chalked up to the long distance between donor and acceptor, which lead to the low charge separation and transportation efficiency, and it also can be seen from the input photon to converted current efficiency (IPCE) curves as shown in Fig. 9. The IPCE value of **P1**, **P2**, **P3** and **P4** are only about 27% at 425 nm, and is very low compared with N719 which could be achieve to 80% at 425 nm [46]. As discussed in the UV-vis absorption spectra section, those two groups of data are proportional development, and the IPCE value is decided by the absorption of light.

4. Conclusion

In this paper, four polymeric metal complexes containing thiophene and diaminomaleonitrile units with Cd(II), Ni(II) were

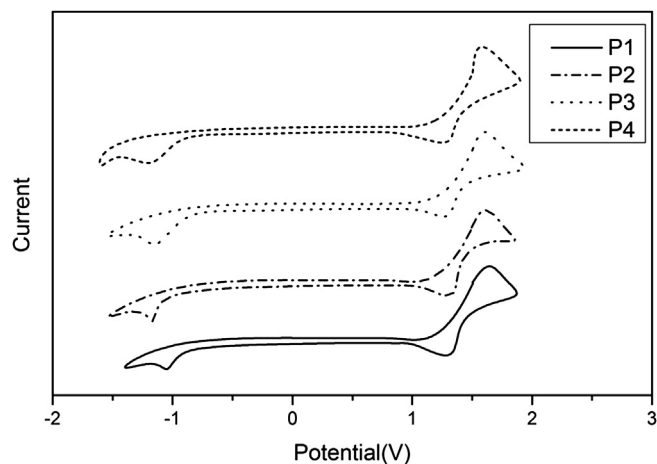


Fig. 8. Cyclic voltammograms for **P1–P4** in DMF/0.1 M [Bu₄N]BF₄ at 100 mV/s.

Table 3
Photovoltaic parameters of devices with sensitizers **P1–P4** in DSSCs at full sunlight (AM 1.5G, 100 mW cm⁻²).

Polymer	Solvent	J_{sc} (mA/cm ²)	V_{oc} (V)	ff (%)	η (%)
P1	DMF	4.38	0.65	69.7	1.98
P2	DMF	4.19	0.61	70.1	1.79
P3	DMF	4.75	0.72	65.8	2.25
P4	DMF	4.52	0.71	65.3	2.10

synthesized, and as sensitizers were used for application. The four materials have showed high stabilities, good open-circuit voltage, fill factor, and power conversion efficiency under simulated AM 1.5G illumination (100 mW cm⁻²). These results strongly predict the importance of their further investigation in DSSCs.

However, there are many challenges to be overcome: J_{sc} and IPCE are very low; at the same time, the electron injection efficiency, light absorption, and the adsorption affinities on the TiO₂ are the main reasons that restrict us to get high η . Because of the low solubility, the polymeric metal complexes cannot be well

dissolved in DMF, and in the UV test and PV test, those complexes could not have more adsorption. Therefore, in order to get good solubility, long alkyls should be introduced in the structure. The absorption region of the polymeric metal complexes is not wide enough, thus they have low IPCE value. For strong adsorption onto the surface of TiO₂, one or two anchoring groups, such as carboxylic acid groups or sulfonic acid groups should also be introduced in the structure [47,48]. For the purpose of improving the solubility and getting better photovoltaic materials, we still have much work to do and we will report the next investigation in the future.

References

- [1] N. Lior, *Energy* 33 (2008) 842.
- [2] D.M. Chapin, C.S. Fuller, G.L. Pearson, *J. Appl. Phys.* 25 (1954) 676.
- [3] A. Hagfeldt, G. Boschloo, L. Sun, L. Klöö, H. Pettersson, *Chem. Rev.* 110 (2010) 6598.
- [4] N.C. John, H. Martnez-Ferrero, A. Viterisi, E. Palomares, *Chem. Soc. Rev.* 40 (2011) 1636.
- [5] M.A. Green, K. Emery, Y. Hishikawa, W. Warta, *Prog. Photovoltaics* 17 (2009) 320.
- [6] B. O'Regan, M. Grätzel, *Nature* 353 (1991) 737.
- [7] I. Chung, B. Lee, J.Q. He, Robert P.H. Chang, Mercouri G. Kanatzidis, *Nature* 485 (2012) 486.
- [8] X.N. Zhang, J. Zhang, Y.Z. Cui, J.W. Feng, Y.J. Zhu, *J. Appl. Polym. Sci.* (2012) 1.
- [9] P.J. Li, J.H. Wu, S.C. Hao, Z. Lan, Q.H. Li, Y.F. Huang, *J. Appl. Polym. Sci.* 120 (2011) 1752.
- [10] M.A. Green, K. Emery, Y. Hishikawa, W. Warta, *Prog. Photovoltaics* 16 (2008) 435.
- [11] M. Grätzel, *Acc. Chem. Res.* 42 (2009) 1788.
- [12] S. Ardo, G.J. Meyer, *Chem. Soc. Rev.* 38 (2009) 115.
- [13] M.K. Nazeeruddin, P. Pechy, M. Grätzel, *Chem. Commun.* (1997) 1705.
- [14] R.K. Lammi, R.W. Wagner, A. Ambrose, J.R. Diers, D.F. Bocian, D. Holten, J.S. Lindsey, *J. Phys. Chem. B* 105 (2001) 5341.
- [15] Y.J. Liu, N. Xiang, X.M. Feng, P. Shen, W.P. Zhou, C. Weng, B. Zhao, S.T. Tan, *Chem. Commun.* (2009) 2499.
- [16] P.Y. Reddy, L. Giribabu, C. Lyness, H.J. Snaith, C. Vijaykumar, M. Chandrasekharan, M. Lakshmi Kantam, J.H. Yum, K. Kalyanasundaram, M. Grätzel, M.K. Nazeeruddin, *Angew. Chem. Int. Ed.* 46 (2007) 373.
- [17] T. Rawling, C. Austin, F. Buchholz, S.B. Colbran, A.M. McDonagh, *Inorg. Chem.* 48 (2009) 3215.
- [18] T. Bessho, S.M. Zakeeruddin, C.Y. Yeh, E. Diau, M. Grätzel, *Angew. Chem. Int. Ed.* 49 (2010) 1–5.
- [19] A. Yella, H.W. Lee, H.N. Tsao, C.Y. Yi, A.K. Chandiran, M.K. Nazeeruddin, E. Diau, C.Y. Yeh, S.M. Zakeeruddin, M. Grätzel, *Science* 334 (2011) 629–633.
- [20] Z.S. Wang, Y. Cui, Y. Dan-Oh, C. Kasada, A. Shinpo, K. Hara, *J. Phys. Chem. C* 111 (2007) 7224.
- [21] B. Liu, W.H. Zhu, Q. Zhang, W.J. Wu, M. Xu, Z.J. Ning, Y.S. Xie, H. Tian, *Chem. Commun.* (2009) 1766.
- [22] R. Chen, X. Yang, H. Tian, X. Wang, A. Hagfeldt, L. Sun, *Chem. Mater.* 19 (2007) 4007.
- [23] A. Baheti, P. Tyagi, K.R.J. Thomas, Y.C. Hsu, J.T. Lin, *J. Phys. Chem. C* 113 (2009) 8541.
- [24] D.P. Hagberg, T. Marinado, K.M. Karlsson, K. Nonomura, P. Qin, G. Boschloo, T. Brinck, A. Hagfeldt, L.J. Sun, *Org. Chem.* 72 (2007) 9550.
- [25] S. Hattori, T. Hasobe, K. Ohkubo, Y. Urano, N. Umezawa, T. Nagano, Y. Wada, S. Yanagida, S. Fukuzumi, *J. Phys. Chem. B* 108 (2004) 15200.
- [26] H.N. Tian, X.C. Yang, R.K. Chen, A. Hagfeldt, L.C. Sun, *Energy Environ. Sci.* 2 (2009) 674.
- [27] N. Koumura, Z.S. Wang, S. Mori, M. Miyashita, E. Suzuki, K. Hara, *J. Am. Chem. Soc.* 130 (2008) 4202.
- [28] S.L. Li, K.J. Jiang, K.F. Shao, L.M. Yang, *Chem. Commun.* (2006) 2792.
- [29] T. Edvinsson, C. Li, N. Pschirer, J. Schöneboom, F. Eickemeyer, R. Sens, G. Boschloo, A. Herrmann, K. Mullen, A. Hagfeldt, *J. Phys. Chem. C* 111 (2007) 15137.
- [30] K. Sayama, K. Hara, N. Mori, M. Satsuki, S. Suga, S. Tsukagoshi, Y. Abe, H. Sugihara, H. Arakawa, *Chem. Commun.* (2000) 1173.
- [31] J. Ohshita, J. Matsukawa, M. Hara, A. Kunai, S. Kajiwarra, Y. Ooyama, Y. Harima, M. Kakimoto, *Chem. Lett.* 37 (2008) 316.
- [32] S. Erten-Ela, M.D. Yilmaz, B. Icli, Y. Dede, S. Icli, E.U. Akkaya, *Org. Lett.* 10 (2008) 3299.
- [33] Y. Hao, X. Yang, J. Cong, H. Tian, A. Hagfeldt, L. Sun, *Chem. Commun.* (2009) 4031.4.
- [34] X.Z. Wang, Q. Wang, L. Yan, W. Wong, K. Cheung, Annie Ng, Aleksandra B. Djurišić, W. Chan, *Macromol. Rapid Commun.* 31 (2010) 861–867.
- [35] W.-Y. Wong, X.-Z. Wang, Z. He, Aleksandra B. Djurišić, Cho-Tung Yip, K.-Y. Cheung, H. Wang, Chris S.K. Mak, W.-K. Chan, *Nat. Mater.* 6 (2007) 521–527.
- [36] C. Li, M.Y. Liu, G.P. Neil, M. Baumgarten, K. Müllen, *Chem. Rev.* 110 (2010) 6817.

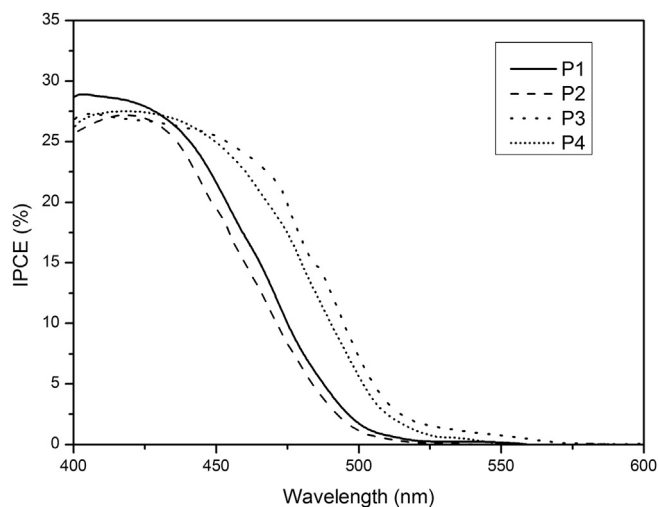


Fig. 9. IPCE plots for the DSSCs based on the four polymeric metal complexes (**P1–P4**) on the ITO glass.

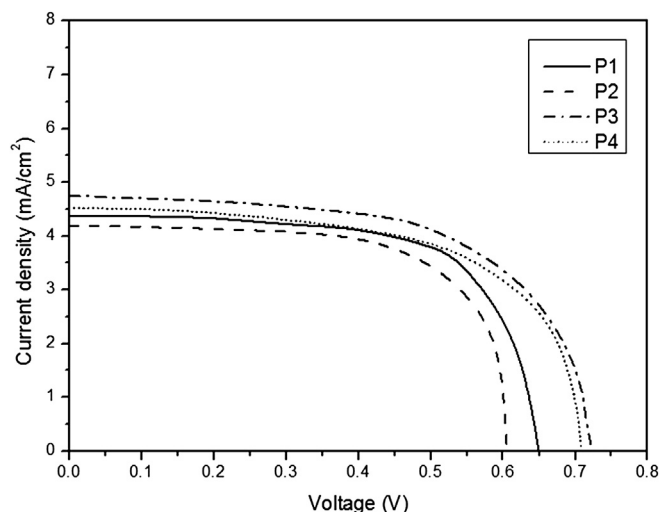


Fig. 10. J - V curves of DSSCs based on dyes (**P1–P4**) under the illumination of AM 1.5, 100 mW cm⁻².

- [37] X.Z. Wang, W. Wong, K. Cheung, M. Fung, Aleksandra B. Djuricic, W. Chan, Dalton Trans. (2008) 5484–5494.
- [38] Z. Fang, A.A. Eshbaugh, K.S. Schanze, J. Am. Chem. Soc. 133 (2011) 3063–3069.
- [39] L.F. Xiao, Y. Liu, Q. Xiu, L. Zhang, L. Guo, H. Zhang, C.F. Zhong, Tetrahedron 66 (2010) 2835–2842.
- [40] L.R. Tsai, Y. Chen, J. Polym. Sci. Part A Polym. Chem. 46 (2008) 70–84.
- [41] S.H. Jin, H.J. Park, J.Y. Kim, K. Lee, S.P. Lee, D.K. Moon, H.J. Lee, Y.S. Gal, Macromolecules 35 (2002) 7532.
- [42] X.Z. Li, W.J. Zeng, Y. Zhang, Q. Hou, W. Yang, Y. Cao, Eur. Polym. J. 41 (2005) 2923.
- [43] C. Ziegler, R. Heck, J. Org. Chem. 43 (1978) 2941–2946.
- [44] Y. Liu, Q. Xiu, L. Xiao, H. Huang, L. Guo, L. Zhang, H. Zhang, S. Tan, C. Zhong, Polym. Adv. Technol. 22 (2011) 2583.
- [45] Y.J. Cheng, S.H. Yang, C.S. Hsu, Chem. Rev. 109 (2009) 5868.
- [46] F. Odobel, E. Blart, M. Lagrée, M. Villieras, H. Boujtita, N.E. Murr, S. Caramori, C.A. Bignozzi, J. Mater. Chem. 13 (2003) 502–510.
- [47] M.K. Nazeerudin, A. Kay, I. Rodicio, R. Humphry-Baker, E. Müller, P. Liska, N. Vlachopoulos, M. Grätzel, J. Am. Chem. Soc. 115 (1993) 6382–6390.
- [48] Z.-S. Wang, F.-Y. Li, C.-H. Huang, J. Phys. Chem. B 105 (2001) 9210.